Applied Catalysis B: Environmental 129 (2013) 39–47

Contents lists available at SciVerse ScienceDirect

Applied Catalysis B: Environmental

journal homepage: www.elsevier.com/locate/apcatb

Biodiesel production from *Jatropha curcas* crude oil using ZnO/SiO_2 photocatalyst for free fatty acids esterification

Grisel Corro[a,*], Umapada Pal[b,1], Nallely Tellez[a]

[a] Instituto de Ciencias, Benemerita Universidad Autonoma de Puebla, 4 sur 104, 72000 Puebla, Mexico
[b] Instituto de Física, Benemerita Universidad Autonoma de Puebla, Apdo. Postal J-48, 72570 Puebla, Mexico

ARTICLE INFO

Article history:
Received 5 March 2012
Received in revised form 5 September 2012
Accepted 6 September 2012
Available online 13 September 2012

Keywords:
Biodiesel
Photocatalytic esterification
Jatropha curcas oil
Heterogeneous photocatalyst

ABSTRACT

We report the production of biodiesel from Mexican *Jatropha Curcas* crude oil (JCCO) by a two step catalytic process. The high content of free fatty acids (FFA) present in JCCO was first esterified with methanol by a photocatalytic process under UV irradiation using ZnO/SiO_2 as the heterogeneous photocatalyst. The solid catalyst was found to be highly active for the heterogeneous photocatalyic esterification of FFA with methanol. The activity of the solid catalyst remained unchanged even after 10 esterification runs, indicating that the heterogeneous photocatalysis is a viable option for FFA esterification reactions for biodiesel production. Transesterification step was catalyzed by NaOH through thermal activation process. Produced biodiesel fulfills all the international requirements for its utilization as a fuel. A probable reaction mechanism for the esterification process is proposed considering the generation of H^+, $CH_3O\cdot$ and R-COOH$^\bullet$ on the photocatalyst surface.

1. Introduction

The use of biodiesel as a replacement of fossil fuels is becoming increasingly popular nowadays due to global energy crisis [1]. Biodiesel, which is mostly produced from vegetable oils, is a mixture of mono-alkyl esters and is perceived to replace the diesel as fuel. Both edible and nonedible vegetable oils can be used as feedstocks in the production of biodiesel. Biodiesel has been produced from a variety of vegetable oil sources such as soybean, sunflower, cottonseed, and others [2–5]. However, the future of utilizing these edible oils is uncertain due to the increased global food demand. There are also issues of deforestation and ecological imbalance while changing the virgin forests and arable lands due to large scale biofuel production [6,7]. Moreover, the use of edible oils for biodiesel increases its production cost substantially.

There are several non-edible oil seed species which are considered to be renewable and sustainable solutions and could be utilized as the source for biofuel production [8–12]. Among them, *Jatropha curcas* is a multipurpose species with considerable potential. It is a drought-resistant tree belonging to the Euphorbiaceae family, native to Mexico. This highly drought-resistant species is adapted to arid and semi-arid conditions. It grows almost anywhere, even on gravelly, sandy and saline soils and is often used for erosion control [13]. The oil extracted from *Jatropha curcas* seeds has good oxidation stability, low viscosity and low freezing point (−5 °C) [14]. In this investigation, we have studied the biodiesel production from Mexican *Jatropha curcas* crude oil (JCCO).

Biodiesel can be blended at any level with petroleum diesel to create a biodiesel blend. It can be used in compression-ignition engines with little or without modification. Biodiesel has suitable viscosity, boiling point, high cetane number; it is simple to use, biodegradable, nontoxic and free of aromatics [8,9].

The most common way to synthesize biodiesel is through transesterification reaction, which refers to a catalytic chemical reaction involving vegetable oil and an alcohol to yield fatty acid alkyl esters (biodiesel) and glycerol (Fig. 1, Reaction (2)) [10–17]. Triglycerides, as the main component of vegetable oil, consist of three long chain fatty acids esterified to a glycerol structure. When triglycerides react with an alcohol, e.g. methanol, the three fatty acid chains are released from the glycerol skeleton and combine with the methanol to yield fatty acid methyl esters (FAME). Glycerol is produced as a by-product.

The yield of FAME from the reaction depends on reaction conditions. The reaction temperature, type and amount of catalyst, alcohol to oil ratio, stirring speed and reaction time are important parameters for the production of biodiesel [18]. Homogeneous catalysts are commonly applied for the transesterification of vegetable oils. Base homogeneous catalysts such as NaOH and KOH are the most active species for this purpose under mild reaction conditions [19].

* Corresponding author. Tel.: +52 22 2295500 7294.
E-mail addresses: griselda.corro@correo.buap.mx (G. Corro), upal@sirio.ifuap.buap.mx (U. Pal).
[1] Tel.: +52 222 2295610.

0926-3373/$ – see front matter © 2012 Elsevier B.V. All rights reserved.
http://dx.doi.org/10.1016/j.apcatb.2012.09.004

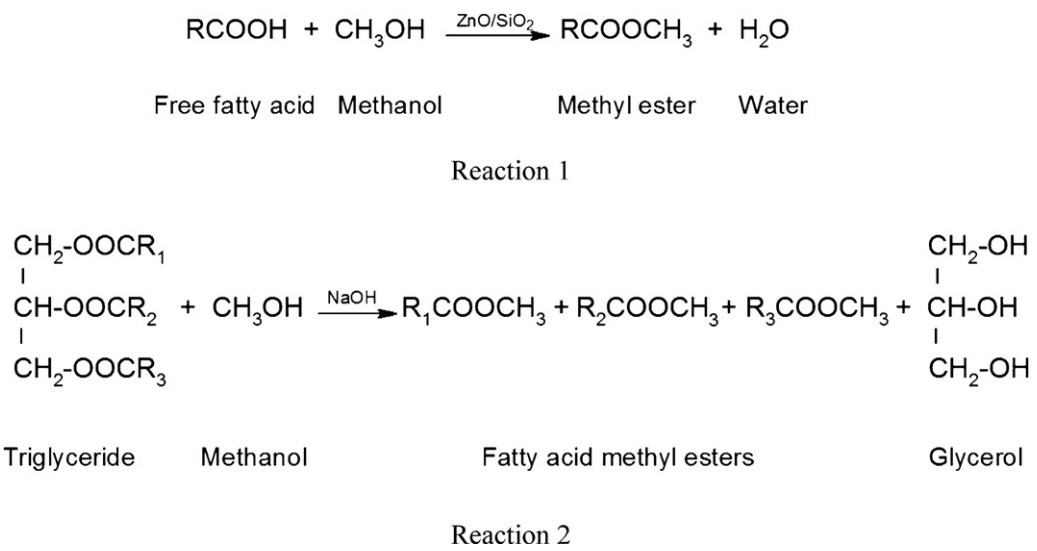

Fig. 1. Biodiesel (fatty acid methyl esters) production by: FFA esterification catalyzed by ZnO/SiO_2 (Reaction (1)); triglycerides transesterification catalyzed by NaOH (Reaction (2)).

An alkali catalyzed process can achieve high purity and high yield biodiesel product in a short time (30–60 min) [20–23]. However, it is very sensitive to the purity of the reactants. It is well known that the moisture and high FFA content of crude vegetable oils are important parameters during catalyzed transesterification reactions [24]. The presence of FFA leads to soap formation and lower yield of biodiesel [21–28]. Well refined vegetable oils with low contents of FFA can be used as the reactant in this process [25]. On the other hand, homogeneous acid catalysts have also been used for this purpose, but they require longer reaction time in comparison with the alkaline-based transesterification processes. Acid catalysts are usually used for oils with high FFA content. However, homogeneous catalysts are difficult to recover and lead to downstream waste treatment, increasing the cost of biodiesel production. The analysis of our unrefined JCCO revealed a high content in free fatty acids (18.05 wt%). Therefore, for the biodiesel production from such high FFA content vegetable oil, generally an acid catalyzed process is preferred, though it would require excess amount of methanol, high pressure (170–180 kPa) and high cost stainless steel equipment [25–27].

In a recent study we applied a combined process for biodiesel production from JCCO, similar to the process proposed by Wang et al. [29,30] for the production of biodiesel from highly acidic waste cooking oil by a two step catalytic process. In this process, first we showed that the use of SiO_2 pretreated with HF as the heterogeneous catalyst in FFA esterification results in a strong decrease of the free fatty acids present in the JCCO. The high activity of this catalyst was explained on basis of the high number of Lewis acid sites present on its surface, which may be responsible for the first step of the FFA esterification reaction. The process proposed for the production of biodiesel was performed at the methanol boiling temperature and is schematized in Fig. 1. The process is advantageous as it does not produce acid wastewater (first step). Moreover, the catalyst could be recovered and reused for 10 runs without being deactivated. However, this process required to be performed at 60 °C under continuous stirring for 2 h.

Several methods have been developed to accomplish the FFA esterification process with alcohols. However, there is no previous report dealing with the photocatalytic esterification of FFA.

ZnO has attracted extensive attention as a heterogeneous photocatalyst for the degradation of organic pollutants in water and air under UV irradiation [31–35]. Moreover, ZnO/SiO_2 has been used as photocatalyst for the photoepoxidation of propene by molecular oxygen [36]. However, as far as our knowledge goes, FFA esterification has never been performed by a heterogeneous photocatalytic process.

In this investigation, we have prepared a ZnO/SiO_2 catalyst, which is of semiconducting nature, having strong absorption band edges in between 235 and 380 nm, suggesting its utilization for photocatalytic esterification of FFA with methanol under UV irradiation. The composite has been utilized for the photocatalytic esterification of FFA present in JCCO with methanol under UV illumination at room temperature.

2. Materials and methods

2.1. Jatropha curcas crude oil (JCCO)

The JCCO was obtained by pressing the Jatropha seeds recollected from the trees growing in a semi-arid region of Puebla, Mexico. The particles remaining in the oil were removed by filtration using an 8 μm filter paper under vacuum conditions. The filtered JCCO was stored in a hermetically sealed PVC can until the analysis of the oil composition and the biodiesel production process were performed (~1 month). The analysis of chemical composition of FFA present in this oil was performed with a gas chromatograph-mass spectrometer HP 6890, provided with a 5973 Network Agilent Technologies detector. The employed standard method in the analysis of the FFA was the NMX-F-017-SCFI-2005. The method consists in a direct injection of the sample in the HP5 column and further identification of the FFA using a free fatty acids mixture provided by Sigma–Aldrich.

2.2. Catalyst

2.2.1. Catalyst preparation

Fused SiO_2 (Baker 99.9%) powders were impregnated with the appropriate amount of aqueous $Zn(NO_3)_2$ solution to obtain a 10 wt% Zn on the SiO_2. The suspension was stirred at room temperature for 1 h. After drying at 120 °C overnight, the catalyst was calcined in air at 500 °C for 12 h, after which it is called as ZnO/SiO_2. A SiO_2 sample without impregnating the $Zn(NO_3)_2$ solution, and a commercial ZnO (Merck 99.9%) powder were calcined in air at 500 °C for 12 h, and used as References

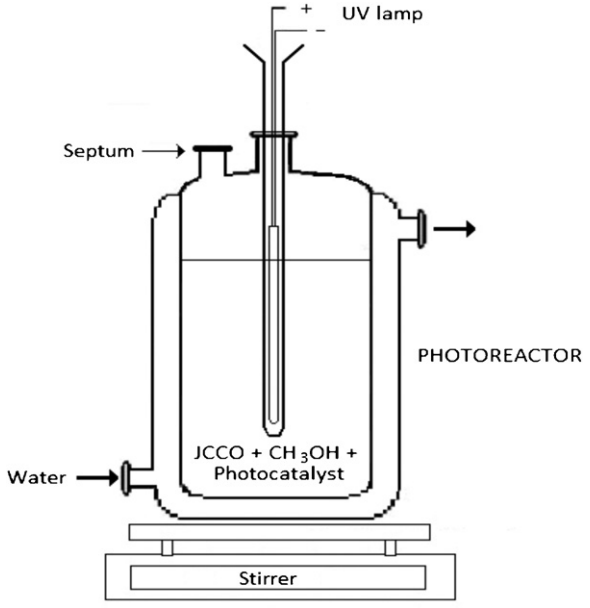

Fig. 2. Schematic layout of the experimental set-up.

2.2.2. Catalyst characterization

Adsorption measurements were performed using a Quantachrome Nova-1000 sorptometer. Total surface areas (S_g) were measured by N_2 physisorption at 77 K using BET analysis methods. The CO_2 and H_2O vapor physisorption over SiO_2 and ZnO/SiO_2 catalysts were determined at 20 °C. The samples (1 g) were degassed at 400 °C for 2 h before recording their physisorption isotherms. After cooling to the desired temperature, the isotherms were performed at a pressure range of 0–6.6 kPa. The technique of back extrapolation of the linear portion of the isotherms to zero equilibrium pressure was used to determine the saturation uptake.

The diffuse reflectance spectrum (DRS) of the composite catalyst was obtained for the dry-pressed disk (~5 mm diameter) samples using a Varian Cary 500 UV-vis spectrophotometer with DRA-CA-30I diffuse reflectance accessory using $BaSO_4$ as standard reflectance sample. The FTIR spectrum of the catalyst was recorded from 800 to 3500 cm^{-1} on a Bruker Vertex 70 spectrometer. For the FTIR measurement, about 1 mg of the composite sample was mixed with about 99 mg of dry KBr and compressed to make a circular pellet of about 5 mm diameter.

The crystallinity and structural phase of the obtained sample were verified through powder X-ray diffraction (XRD) technique using the Cu Kα source (λ = 1.5406 Å) of a Bruker D8 Discover diffractometer.

2.3. Process for biodiesel preparation from JCCO

2.3.1. First step: FFA photoesterification with methanol

Photocatalytic experiments were carried out in a photoreactor newly designed and built in our laboratory. The detail schematic drawing of the experimental set-up is shown in Fig. 2. UV radiation was provided with a 3 W pen-ray lamp which emitted Mercury spectrum with the primary energy at 254 nm and secondary energies at 184.9, 312.5, 386.0, 404.7, and 435.8 nm. The lamp was immersed fully into the reaction mixture. Temperature rise of the reaction mixture was prevented by utilizing a temperature controlled circulating-water cell in order to avoid any thermal activation on the esterification reaction. The reactor was provided with an internal magnetic stirrer which generated a strong liquid rotation leading to a homogeneous irradiation of the whole reacting mixture.

2.3.1.1. Optimization of reaction conditions. The photocatalytic experiments were performed at 20 °C. The reactants were methanol (Aldrich, 99%) and JCCO. The methanol/JCCO molar ratio was 12/1, according to the optimum value determined in our previous investigation [29]. The catalyst concentration range used was 2–20 wt% of the initial JCCO mass. The speed of stirring was 400 rpm. The photocatalytic reaction was carried out under UV irradiation and was allowed to proceed for different reaction times. A blank experiment was run without the catalyst under the same experimental conditions. Another blank experiment was run with a catalyst concentration 10 wt% of the initial JCCO mass under the same conditions but in the absence of UV irradiation.

In order to identify the active sites of the ZnO/SiO_2 catalyst for the photo-esterification reaction, we studied separately the photocatalytic activity of ZnO (Aldrich 99%), SiO_2 (Baker 99.9%) and metallic Zn (Aldrich 99%). These reactions were performed under the same conditions as for the ZnO/SiO_2 catalyst using a catalyst mass of 10 wt% of the initial JCCO mass.

After the desired time of reaction, the mixture was left to settle to separate into two layers. The lower oil layer was composed of methyl esters produced by the FFA esterification, the unreacted triglyceride (that was further subjected to the transesterification reaction) and the solid, insoluble catalyst that was recovered for further use. The upper layer was a mixture of methanol and the water produced during Reaction (1) (Fig. 1).

In order to determine the presence of leached Zn from the catalyst, the upper and lower layers of the reacted mixture were analyzed by atomic absorption spectrometry. Results revealed a Zn concentration lower than 2 ppm in both the samples. This low level indicates that the leaching of Zn occurs during FFA esterification is low.

The durability test of the catalyst was performed by repeating the esterification reaction 10 times with the same sample under the following conditions: the catalyst concentration was 2 wt% of the initial JCCO mass, the speed of stirring was 400 rpm, the time of UV irradiation was 1 h. Under these conditions only about 15% conversion of the FFA could be achieved. This stability study was conducted at low FFA conversion using a low catalyst concentration to prevent an excess of catalyst which might result in a non-apparent deactivation and a conversion which would still be high. Catalyst separated from the previous reaction mixture was used for the next cycle without further washing or any other pretreatment.

2.3.1.2. Acid number determination. The acid number of the initial JCCO or after the FFA esterification reaction was determined according to the ASTM D 664 international standard method. This method consists in dissolving a test sample in a mixture of diethyl ether and ethanol and a further titration with a KOH solution. The end point was determined with a pH-meter equipped with glass and calomel electrodes.

The acid value A is determined according to Eq. (2):

$$A = \frac{56.1 \times V \times c}{m} \quad (2)$$

where V = volume, in milliliters of standard volumetric potassium hydroxide solution used, c = concentration, in moles per liter, of the standard volumetric potassium hydroxide solution used, m = mass, in grams of the test portion, 56.1 = molecular mass of potassium hydroxide.

2.3.1.3. Determination of the %conversion of FFA. The conversion of the FFA is defined as the fraction of FFA that reacted during the esterification reaction with methanol. The conversion of FFA ($\%C_{FFA}$)

Table 1
FFA composition of JCCO.

Free fatty acid	wt%
Oleic acid	8.12
Linoleic acid	6.33
Palmitic acid	2.73
Linolenic acid	0.15
Other acids	0.72
Total FFA content	18.05

was determined from the acid number ratio using the following equation:

$$\%C_{FFA} = \frac{A_i - A_f}{A_i} \times 100 \quad (3)$$

where A_i is the initial acid number of the JCCO and A_f is the final acid number of the JCCO after the FFA esterification reaction.

2.3.2. Second step: alkali catalyzed transesterification of JCCO

2.3.2.1. Reaction conditions. The mixture of the esterified FFA and the unreacted triglyceride was dried under stirring at 110 °C for 2 h and transferred to the photoreactor. The estimated water content was 0.158% as determined by the Karl Fisher method (ISO 12937 Standard) [37]. Six times the stoichiometric amount of methanol required for total conversion of triglyceride and 1.0 wt% of NaOH were added as proposed by Zhang et al. [25]. The photocatalytic reaction was carried out under UV irradiation under stirring at 400 rpm and was allowed to proceed for different reaction times. However, at 20 °C the reaction proceeded at a very slow rate. Thus, the triglycerides transesterification reactions with methanol were performed without UV irradiation, at 60 °C for 20 min under stirring at 400 rpm. The mixture was left to settle overnight to separate in two layers. The upper layer was the FAME and the lower layer was the mixture of methanol, water and glycerol as indicated in Reaction (2) (Fig. 1). The FAME obtained was washed with hot water (80 °C) and dried under stirring at 100 °C for 2 h.

2.3.2.2. Chemical analysis of the produced biodiesel. The FAME content in the obtained biodiesel was estimated through GC analysis according to the EN 14103 test method. This test was performed to verify that the ester content of FAME is greater than 90% (m/m) and that the linolenic acid content is between 1% (m/m) and 15% (m/m). A methyl heptadecanoate solution was added to the biodiesel sample prior to the GC analysis. Further identification of the methyl esters was performed using the NLEA FAME Mix standard provided by Restek.

The determination of the free, bound, and total glycerin, and mono, di-, and triglycerides, was performed according to the ASTM D 6584 test method, using the EZStart Chromatography Software provided by Shimadzu Co. In this procedure, the sample was analyzed after silyating with N-methyl-N-trimethylsilyltrifluoracetamide. For calibration, two internal standards and four reference materials were utilized. The contents of mono-, di-, and triglycerides were determined by comparing with monoolein, diolein, and triolein standards respectively. Average conversion factors were applied to the mono-, di-, and triglycerides to calculate the bonded glycerin content in the sample.

3. Results and discussion

3.1. JCCO analysis

The FFA chemical composition analysis performed by GC–MS of the JCCO is reported in Table 1. This table shows 18.05% content of FFA in the JCCO used in this investigation.

Table 2
Catalyst characterization data.

Catalyst	Specific surface area ($m^2\,g^{-1}$)	Adsorption saturation uptake ($mmol\,g^{-1}$)	
		CO_2 (20 °C)	H_2O (20 °C)
ZnO/SiO_2	160	0	0
SiO_2	180	0	0
ZnO	35	0	0

3.2. Catalysts characterization

The catalyst characterization data is summarized in Table 2. The results obtained from the physisorption isotherms show no CO_2 or H_2O uptakes at 20 °C.

These results suggest that at 20 °C, the surface of the catalyst can remain free of these molecules, thus the adsorption of the reactants during esterification reactions (20 °C) may be easily performed. Moreover, the FTIR spectrum obtained from the ZnO/SiO_2 (Fig. 3c) catalyst revealed no absorption band either at 3335 cm^{-1} or at 1400 cm^{-1} corresponding to water, neither the typical 2360 cm^{-1} band due to CO_2 absorption. The results are expected as we used amorphous fused silica for the preparation of the composite catalysts. Used fused SiO_2, which presents a low surface area (180 m^2/g) may adsorb CO_2 or H_2O at a much lower rate in comparison with silica gel, whose high surface area (~800 m^2/g) allows it to adsorb water readily.

FTIR transmittance spectra of pure ZnO (Merck, 99%), fused silica and ZnO/SiO_2 composite are presented in Fig. 3. It can be observed that the FTIR spectrum obtained from ZnO revealed only a signal at around 532 cm^{-1} which corresponds to the (E_2-high + E_2-low) multiphonon vibration of wurtzite ZnO [38]. The fused silica sample revealed its characteristic absorption bands near about 804 and 1070 cm^{-1} which correspond to the Si—O—Si bending and Si—O—Si stretching modes, respectively [39]. The shifts of the stretching mode towards higher frequency (with respect to the standard values of 1050 cm^{-1}) might be due to the adsorption of water or change in stress [40]. On the other hand, apart from the absorption bands corresponding to SiO_2 and ZnO, the ZnO/SiO_2 composite revealed four closely spaced bands at around 871, 905, 932, and 976 cm^{-1}, which are close to the characteristic FTIR signals of zinc silicate (1081, 1005, 937, and 800 cm^{-1}) [41–43]. It must be noted

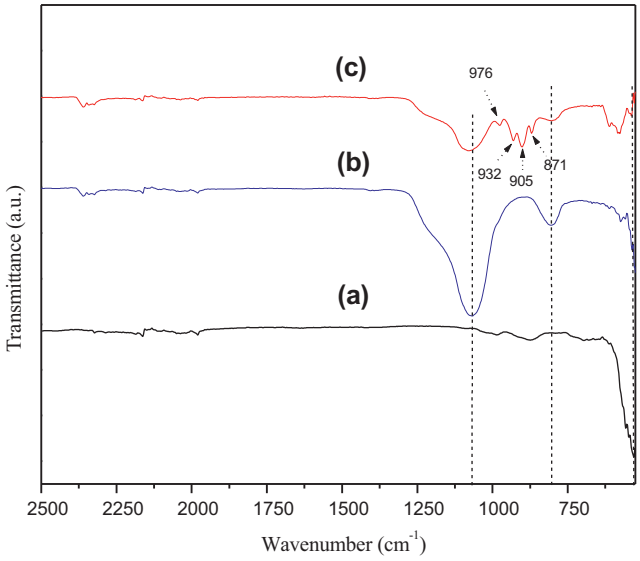

Fig. 3. FTIR spectra of (a) ZnO, (b) fused SiO_2, and (c) ZnO/SiO_2.

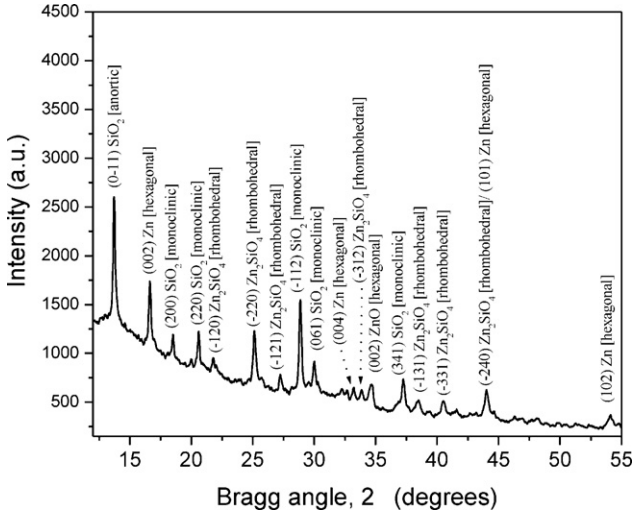

Fig. 4. XRD pattern of the ZnO/SiO_2 catalyst after calcinations at 500 °C for 2 h in air. Increasing background at the lower Bragg angles indicates the partial amorphous nature of the sample.

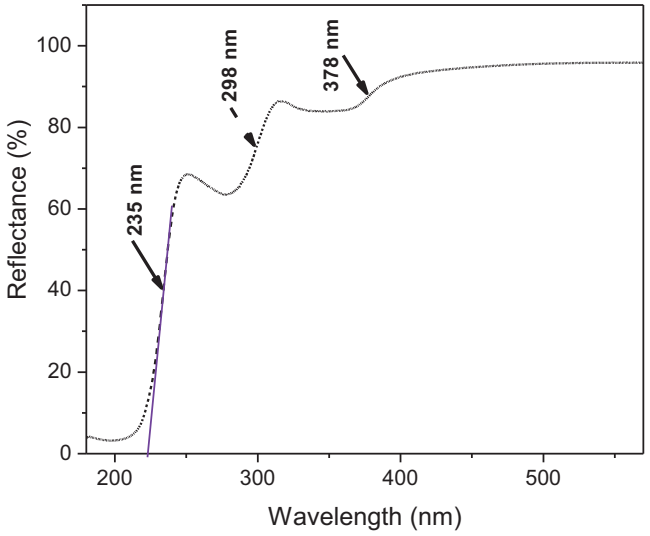

Fig. 5. Diffuse reflectance spectrum of the ZnO/SiO_2 catalyst after calcinations at 500 °C for 2 h in air. Three clear absorption edges appearing due to the composite nature of the catalyst are marked by arrows.

that while the signals correspond to both SiO_2 and ZnO are shifted towards higher wave number in the spectrum of the ZnO/SiO_2 composite, the signals correspond to zinc silicate are situated at lower wave numbers with respect to the reported values. Such spectral shifts in the composite sample are expected due to the composite nature of the sample, as well as non-stoichiometric nature of the components (ZnO, SiO_2, and Zn_2SiO_4). Presence of elemental zinc, as revealed from the XRD spectrum of the composite indicates high oxygen vacancy content in the sample. Additionally, formation of ZnO from zinc during the calcinations process might also have created severe oxygen vacancies in SiO_2.

XRD pattern of the ZnO/SiO_2 catalyst is shown in Fig. 4. In this figure it can be seen that the composite catalyst is the mixture of SiO_2 in monoclinic (JCPDF #891667) and anortic (JCPDF #891812) phases, Zn_2SiO_4 in rhombohedral phase (JCPDF #850453), ZnO in wurtzite phase (JCPDF #361451), and Zn in hexagonal phase (JCPDF #870713). Therefore, though we designated the air annealed composite sample as ZnO/SiO_2, apart from silica in two structural phases, it contains zinc both in oxidized and elemental phases. Presence of Zn, ZnO and SiO_2 in the composite catalyst is very clear from its DRS (Fig. 5).

The diffuse reflectance spectrum of the sample presented in Fig. 5 reveals three clear absorption edges at about 235, 298, and 378 nm wavelengths, which correspond to the absorption edges of Zn_2SiO_4, plasmonic resonance absorption edge of Zn clusters, and absorption edge of ZnO, respectively. While the band edge at about 235 nm corresponds to the strong absorption of zinc silicate with band gap around 5.3 eV, the absorption edge at about 298 nm corresponds to a combined absorption of Zn^{+2} ions Zn^0 clusters [43,44]. On the other hand, the absorption edge near 378 nm corresponds to the near band edge absorption of ZnO [38]. The DRS spectrum of the composite catalyst clearly demonstrates the presence of zinc silicate, ZnO, Zn^{+2} ions and Zn^0 in it.

3.3. FFA photo-esterification over ZnO/SiO_2

To determine the optimal conditions for FFA esterification reaction photocatalyzed by ZnO/SiO_2, we examined the effects of the photocatalyst/JCCO mass ratio and the UV-irradiation time. Fig. 6 shows the evolution of the FFA % conversion as a function of the UV-irradiation time for different catalyst/JCCO mass ratios at 20 °C keeping the methanol/JCCO mass ratio fixed (12/1). Used values of catalyst/JCCO mass ratios were selected considering the optimum values determined in our previous study of the esterification of FFA in JCCO using solar radiation as energy source [29]. From Fig. 6, we can see that in absence of UV irradiation, the FFA % conversion at 20 °C is very low, even after 8 h of reaction, indicating that FFA esterification does not take place over the catalyst at this temperature without UV irradiation. On the other hand, a very low FFA % conversion even after 8 h of UV irradiation at 20 °C indicates that the homogeneous photoesterification of FFA with methanol does not take place.

The FFA % conversion increased with UV irradiation time for all the studied catalyst/JCCO mass ratios. At the initial stage of the reaction, the conversion rate increased with the increase of catalyst/JCCO mass ratio. At high catalyst/JCCO mass ratio, the FFA % conversion is high even for low irradiation time. These results suggest that the esterification of FFA with methanol takes place over ZnO/SiO_2 catalyst through a heterogeneous photocatalytic process. For the catalyst/JCCO mass ratios higher than 10%, the reaction rate does not increase considerably. The saturation of reaction rate can be understood considering that high catalyst content in the reaction mixture does not allow all the catalyst particles to be illuminated. In fact a very high percentage of FFA conversion (96%) could be

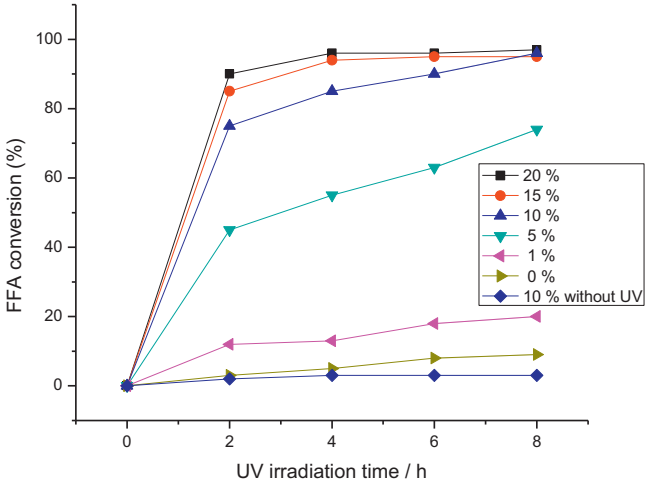

Fig. 6. Effect of UV irradiation time on the FFA % conversion catalyzed by different ZnO/SiO_2/JCCO mass ratios at a fixed methanol/JCCO molar ratio 12/1.

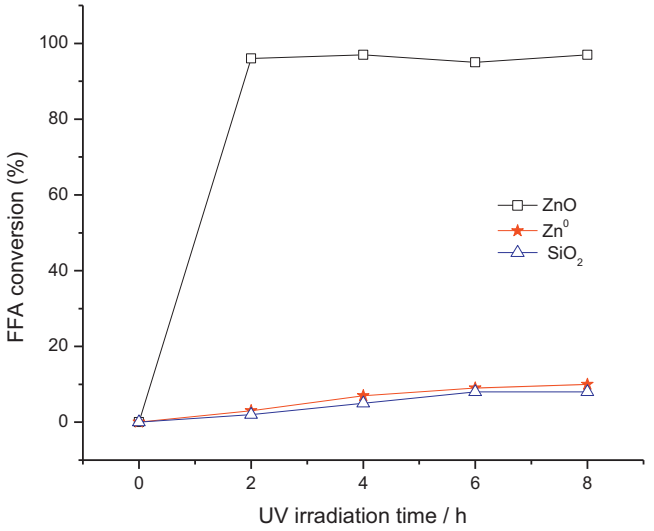

Fig. 7. Effect of UV irradiation time on the FFA % conversion catalyzed by ZnO, Zn^0, and SiO_2 (10 wt% of JCCO mass and a fixed methanol/JCCO molar ratio 12/1).

obtained on irradiating the reaction mixture only for 4 h when a catalyst/JCCO mass ratio of 15% was utilized. Further increase of catalyst/JCCO mass ratio (20%) and further increase in reaction time resulted in only a slight increase of the FFA conversion. Thus, the conditions for the photoesterification process were fixed to a catalyst/JCCO mass ratio of 15% and 4 h of reaction time, keeping the methanol/JCCO mass ratio fixed (12/1).

The results obtained from the XRD and DRS spectroscopies showed the presence of ZnO, Zn^{+2} ions and Zn^0 in the ZnO/SiO_2 composite catalyst. Fig. 7 shows the evolution of the FFA % conversion with UV-irradiation time over ZnO, metallic Zn and SiO_2. From the figure, it can be clearly seen that metallic Zn and SiO_2 were inactive for FFA photo-esterification. Very low FFA % conversion values were observed, even after 8 h of UV-irradiation. However, for the reaction over ZnO, a very high value of FFA % conversion was determined during the first UV-irradiation hour (96%). These results suggest that active sites on the ZnO/SiO_2 composite catalyst prepared in this investigation may be the ZnO particles at the surface of the composite. This assumption is supported by the results we obtained from the photo-esterification of FFA using ZnO/Al_2O_3 performed in similar reaction conditions as in the present work. While Al_2O_3 did not present activity for this reaction, the ZnO/Al_2O_3 showed 85% FFA conversion (unpublished results).

Though the FFA could be photo-esterified using ZnO alone, a technical problem arises with its use as photocatalyst due to a strong disaggregation of the solid in the reacting mixture. Separation of the catalyst and the liquid phase was difficult to perform, and a high content of fine ZnO particles was observed in the final esterified mixture.

A basic mechanism of photocatalytic reaction on the generation of electron–hole pair and its destination is as follows: when a heterogeneous photocatalyst (semiconductor) is illuminated by light stronger than its band gap energy, electron–hole pairs diffuse out to the surface of the photocatalyst and participate in the chemical reaction, interacting with surrounding molecules. The free electrons (e^-) and holes (h^+) transform the surrounding molecules into free radicals [45]. The surrounding molecules might be the methanol and free fatty acids present in JCCO during a heterogeneous photocatalytic esterification of FFA with methanol under UV irradiation.

Now, in a study of hydrogen production by photocatalytic reforming of methanol on Au/TiO_2 catalyst [46], it has been proposed that methanol is oxidized by a positive hole generated during the catalyst irradiation according to the following reaction:

$$CH_3OH + h^+ \rightarrow CH_3O^\bullet + H^+ \quad (1)$$

The generation of $CH_3O^\bullet$ radicals has also been proposed by Cui et al. [47] to explain the hydrogen production by photocatalysis of methanol vapor over Ti-beta.

Based on the photolytic esterification process of carboxylic acids with alcohols reported by Hwu et al. [48], we believe that a possible reaction between the FFA present in JCCO and the free electrons (e^-) generated over our catalyst on UV irradiation takes place. The possibilities of generation of $CH_3O^\bullet$ radicals by the positive holes (h^+) and the reaction between FFA and the photo-generated free electrons (e^-) suggest that the process of FFA esterification with methanol can be performed under UV irradiation in the presence of a heterogeneous photocatalyst.

The effect of UV irradiation on the FFA esterification process can be understood from the schematic energy transfer diagram presented in Fig. 8. The UV-induced esterification process proceeds in the following steps:

1. Transfer of methanol (CH_3OH) and FFA (HOOC-R) to the surface of ZnO/SiO_2 photocatalyst. This step may be accelerated by the strong stirring conditions in the reactor.
2. Adsorption of methanol and FFA on the photocatalyst surface. FFA may be mainly adsorbed at the Zn^{+2} surface sites which may act as Lewis acid sites, and methanol may be mainly adsorbed on the lattice oxygen atoms on the surface which may act as Lewis basic sites [49,50].
3. Reaction in the adsorbed phase follows the following steps:
   - UV photon absorption by ZnO/SiO_2 photocatalyst, mainly by ZnO sites, and generation of photon-induced electrons e^- and holes h^+.
   - Due to high oxidative potential, the photo-generated holes (h^+) may react with CH_3OH adsorbed on the catalyst surface, producing hydrogen ions (H^+) and $CH_3O^\bullet$ radicals in a similar way as it has been proposed for the hydrogen production by photocatalytic reforming of methanol [46,47]:

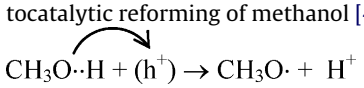

   - At the same time $^\bullet$HOOC-R radicals might be formed by oxidation of HOOC-R adsorbed at the catalyst surface reacting with photogenerated e^-, (in a similar way as O_2 reacts with photogenerated e^- to form superoxide species $^\bullet O_2$):

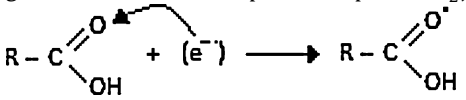

4. The generated/formed H^+, $^\bullet$O-CH_3, and $^\bullet$HOOC-R subsequently would react to form the intermediates and final products, as shown in the proposed reaction scheme in Fig. 9.
5. Desorption of the fatty acid methyl ester and the water produced during the FFA photoesterification reaction.
6. Transfer of the products from the interface region to the liquid phase. This step may be accelerated by the strong stirring conditions in the reactor.

In Fig. 10, the FFA esterification evolution over ZnO/SiO_2 as a function of the number of runs at the optimal determined reaction conditions is presented. The figure shows that after 10 runs, the activity of the catalyst for FFA esterification remains almost unaltered. On the other hand, the above result also suggests that the amount of catalyst during the reaction remains unchanged, i.e. not dissolved in the H_2O produced during esterification (Fig. 1, Reaction (1)) as it has been reported previously for other catalysts such as CaO [51]. Moreover, many different heterogeneous

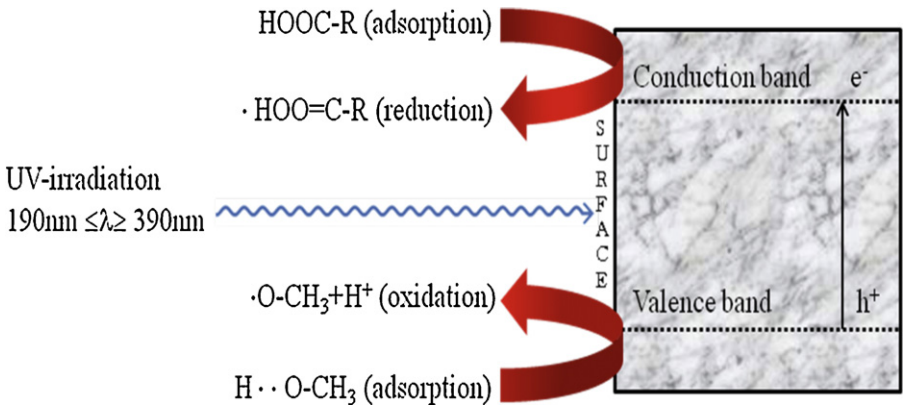

Fig. 8. Proposed mechanism to explain the effect of the UV irradiation on the FFA esterification rate over ZnO/SiO_2.

catalysts have been developed to utilize in the production of biodiesel. For example, CsX zeolites, anionic clays, calcium carbonate rock, EST-10, LiCaO and $Na/NaOH/Al_2O_3$ have been found to be efficient heterogeneous catalysts for this purpose [52–56]. However, either they are quite expensive, or complicated to prepare, which limits their industrial application. On the other hand, our ZnO/SiO_2 photocatalyst is efficient and cheap, active at room temperature for the process described in this work, easy to recover, and highly promising for commercial biodiesel production.

3.4. Alkali catalyzed transesterification of JCCO

We tried to perform the photocatalytic transesterification of triglycerides present in JCCO under UV irradiation under stirring at 400 rpm for different reaction times. However, at 20 °C the reaction proceeded at a very slow rate. Even after 40 h of UV irradiation, high values of mono, di- and triglycerides were detected in the final reaction mixture (results not shown). These results suggested that thermal activation is required to increase the effective interactions between methanol and triglycerides. Thus, the triglycerides

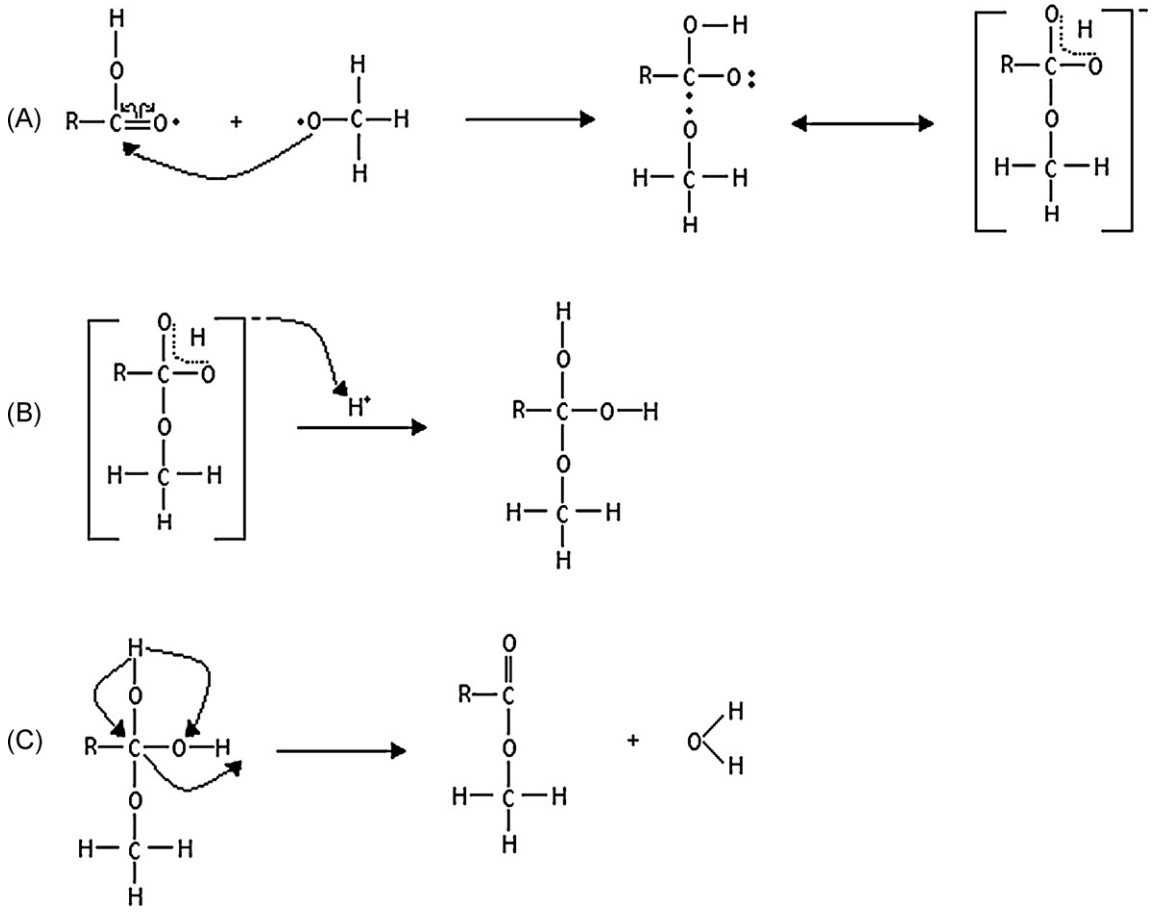

Fig. 9. Reaction scheme for H^+, $^{\bullet}O\text{-}CH_3$, and $^{\bullet}HOOC\text{-}R$ interactions leading to final products: $RCOO\text{-}CH_3$ and H_2O. (A) The $^{\bullet}O\text{-}CH_3$ radical reacts with the carbonyl group of the $^{\bullet}HOOC\text{-}R$ radical. (B) The H^+ reacts with the unstable tetrahedral intermediate. (C) The tetrahedral intermediate breaks down to fatty acid methyl-ester ($RCOO\text{-}CH_3$) and water.

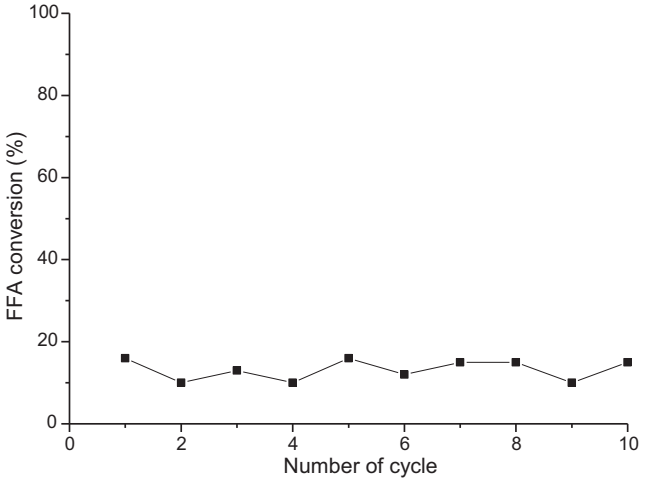

Fig. 10. FFA % conversion at different reaction cycles over ZnO/SiO_2 catalyst (2 wt%).

Table 3
Fatty acid methyl esters composition of the biodiesel obtained from JCCO determined by gas chromatography (according to the EN 14103 test method).

Methyl ester	wt%
Methyl linoleate	19.0
Methyl sterate	21.4
Methyl palmitate	22.7
Methyl oleate	35.1
Other compounds	1.8
Total	100

transesterification reactions with methanol were performed without UV irradiation, at 60 °C for 20 min under stirring at 400 rpm.

The transesterification reaction of the triclycerides in the JCCO after the FFA photoesterification process (using ZnO/SiO_2 catalyst in methanol) was performed with the NaOH homogeneous catalyst. Tables 3 and 4 report the physical and chemical characteristics of the produced biodiesel determined from gas chromatography analysis. The composition of generated FAME in the biodiesel are listed in Table 3 and the contents of monoglyceride, diglyceride, triglyceride, free, bound and total glycerin in the final product, determined according to the ASTM D 6584 test method, are reported in Table 4. It can be observed that the obtained biodiesel contains very low percentage of these undesired molecules.

The values presented in Tables 3 and 4 show that the process proposed in this investigation can generate biodiesel of high purity that meets the quality demands for its use and commercialization. The process presented in the present work prevents the generation of waste water, use of excess methanol, high pressure, and avoids the use of high cost stainless steel equipments frequently used for the FFA esterification process of JCCO.

Table 4
Properties of the biodiesel obtained from JCCO, using ZnO/SiO_2 as photocatalyst for esterification of FFA and NaOH as catalyst for transesterification of triglycerides with methanol.

Property	Biodiesel produced by this method	Limiting allowed values
Density at 15 °C	870 kg m^{-3}	(860–900) kg m^{-3}
Kinematic viscosity at 40 °C	3.9 mm^2 s^{-1}	(3.5–5.0) mm^2 s^{-1}
Acid number	0.37 mg KOH g^{-1}	(0.0–0.5) mg KOH g^{-1}
Ester content	96.2 wt%	(96.5–100) wt%
Esters with >4 double bonds	0 wt%	(0.0–1.0) wt%
Esters from linolenic acid	0.01 wt%	(0.0–12.0) wt%
Monoglyceride	0.50 wt%	(0.0–0.8) wt%
Diglyceride	0.15 wt%	(0.0–0.2) wt%
Triglyceride	0.10 wt%	(0.0–0.2) wt%
Free glycerin	0.01 wt%	(0.0–0.02) wt%
Bound glycerin	0.10 wt%	(0.0–0.23) wt%
Total glycerin	0.11 wt%	(0.0–0.25) wt%

Results presented in this work demonstrate the possibility of performing the FFA esterification with methanol through a heterogeneous photocatalytic process. To the best of our knowledge, this is the first time that such process has been undertaken under the presented reaction conditions. In this work, we investigated the photocatalytic performance of ZnO/SiO_2, and the possibility of FFA photoesterification with methanol over this catalyst has been demonstrated. However, the possibility of utilization of other semiconductors as active photocatalysts for the photoesterification of FFA cannot be discarded. The results presented in this article open up a new research field for further investigations to improve biodiesel production.

4. Conclusions

We have demonstrated the use of ZnO/SiO_2 as a heterogeneous photocatalyst for efficient esterification of FFA present in JCCO, which is the essential step for the production of biodiesel from non edible vegetable oils. The catalyst is reusable, without decreasing its catalytic efficiency even after 10 cycles of utilization. The catalyst does not get deactivated by hydration or carbonation during esterification reaction. After photoesterification of FFA, the transesterification reaction of triglycerides (present in the JCCO) was catalyzed by NaOH, producing a high quality biodiesel that meets the international demands for its use and commercialization. The use of heterogeneous photocatalytic process at room temperature can be a new way to perform the esterification of FFA in vegetable oils for the efficient production of biodiesel.

Acknowledgements

The authors acknowledge the financial supports from FOMIX-CONACYT, Puebla (Grant # 130389 and 179988), CONACYT, Mexico (Grant # 151767) and VIEP, BUAP (Grant # NAT 38-2011) extended to perform this research work.

References

[1] R. Luque, J.C. Lovett, B. Datta, J. Clancy, J.M. Campelo, A.A. Romero, Energy & Environmental Science 3 (2010) 1706–1721.
[2] M.L. Schlick, M.A. Hanna, J.L. Schinstock, Transactions of ASAE 31 (1988) 1345–1349.
[3] G. Antolin, F.V. Tinaut, Y. Briceno, Bioresource Technology 83 (2002) 111–117.
[4] H. Fukuda, A. Kondo, H. Noda, Bioscience and Bioengineering 92 (2001) 405–416.
[5] Y.C. Sharma, B. Singh, S.N. Upadyay, Fuel (2008) 2355–2373.
[6] R.A. Buttler, http://www.news.monogabay.com/2006/0425-oil.palm.html, 2006.
[7] R. Luque, L. Herrero-Davila, J.M. Campelo, J.H. Clark, J.M. Hidalgo, D. Luna, J.M. Marinas, A.A. Romero, Energy & Environmental Science 1 (2008) 542–564.
[8] B. Kegl, Fuels Energy 20 (2006) 1460–1470.
[9] J.C. Pasqualino, D. Montane, J. Salvado, Biomass and Bioenergy 30 (2006) 874–879.
[10] Y.C. Sharma, B. Singh, Fuel (2010) 1470–1474.
[11] A. Kumar, S. Sharma, Industrial Crops and Products 28 (2008) 1–10.
[12] J. Xue, T.E. Grift, A.C. Hansen, Renewable and Sustainable Energy Reviews 15 (2011) 1098–1116.
[13] K. Openshaw, Biomass and Bioenergy 19 (2000) 1–15.
[14] L.C. Meher, V.D. Sagar, S.N. Naik, Renewable and Sustainable Energy Reviews 10 (2006) 248–268.
[15] K. Narasimharao, D.R. Brown, A.F. Lee, A.D. Newman, P.F. Siril, S.J. Tavener, K. Wilson, Journal of Catalysis 248 (2007) 226–234.
[16] B.M.E. Russbueldt, W.F. Hoelderich, Journal of Catalysis 271 (2010) 290–304.
[17] M. Lopez-Granados, A.C. Alba-Rubio, F. Vila, D. Martin-Alonso, R. Mariscal, Journal of Catalysis 276 (2010) 229–236.
[18] P.K. Sahoo, L.M. Das, Fuel 88 (2009) 1588–1594.
[19] B. Smith, H.C. Greenwell, Energy & Environmental Science 2 (2009) 262.
[20] P.R. Muniyappa, S.C. Brammer, H. Noureddini, Bioresource Technology 56 (1996) 19.
[21] A.P. Vyas, J.L. Verma, R. Subrehmanyam, Fuel 89 (2010) 1–9.

[22] M. Dorado, E. Ballesteros, F.J. Lopez, Energy & Fuels 18 (2004) 77–83.
[23] M. Canakci, J.V. Gerpan, Transactions of the American Society of Agricultural Engineers 44 (2001) 1429–1436.
[24] J. Dupont, P.A.Z. Suarez, M.R. Meneghetti, S.M.P. Meneghetti, Energy & Environmental Science 2 (2009) 1258–1265.
[25] Y. Zhang, M.A. Dube, D.D. McLean, Bioresource Technology 86 (2003) 1–16.
[26] M.I. Al-Widyan, A.O. Al-Shyoukh, Bioresource Technology 85 (2002) 253–256.
[27] G.M. Tashtoush, M.I. Al-Widyan, A.O. Al-Shyoukh, Energy Conversion and Management 45 (2004) 2697–2711.
[28] S.V. Ghadge, H. Raheman, Biomass and Bioenergy 28 (2005) 601–605.
[29] G. Corro, N. Tellez, E. Ayala, A. Martinez-Ayala, Fuel 89 (2010) 2815–2821.
[30] Y. Wang, S. Ou, P. Liu, F. Xue, S. Tang, Journal of Molecular Catalysis A: Chemical 252 (2006) 107–115.
[31] S. Chakrabarti, B.K. Dutta, Journal of Hazardous Materials B 112 (2004) 269–278.
[32] G.P. Fotou, S.E. Pratsinis, Chemical Engineering Communications 151 (1996) 251–260.
[33] M.I. Curridal, R. Comparelli, P.D. Cozli, G. Mascolo, A. Agostiano, Materials Science and Engineering C 23 (2003) 285–292.
[34] S.B. Park, Y.C. Kang, Journal of Aerosol Science 28 (1997) S473–S478.
[35] R.Y. Hong, T.T. Pan, J.Z. Qian, H.Z. Li, Chemical Engineering Journal 119 (2006) 71–79.
[36] H. Yoshida, T. Shimizu, C. Murata, T. Hattori, Journal of Catalysis 220 (2003) 226–232.
[37] BS EN ISO 12937: 2000, Petroleum products, Determination of water, Coulometric Karl Fisher titration method.
[38] G. Muñoz Hernandez, A. Escobedo Morales, U. Pal, Crystal Growth & Design 9 (2009) 297–303.
[39] F.L. Galeenar, Physical Review B 19 (1979) 4292–4299.
[40] R. Hoffman, J.G.F. Westheim, I. Powell, P.J. Gellings, Surface and Interface Analysis 24 (1996) 1–8.
[41] M.R. Bisengalieva, L.P. Ogordova, M.F. Visasina, Russian Journal of Physical Chemistry A 84 (2010) 1481–1488.
[42] http://www.ruff/Hemimorphite, R040117 – RRUFF Database Raman, X-ray, Infrared, and Chemistry.mht.
[43] Q.Y. Zang, K. Pita, C.H. Kam, Journal of Physics and Chemistry of Solids 64 (2003) 333–341.
[44] G. Canizal, P.S. Schabes-Retchkiman, U. Pal, H.B. Lu, J.A. Ascencio, Materials Chemistry and Physics 97 (2006) 321–329.
[45] Y.J. Jang, C. Simar, T. Ohm, Materials Research Bulletin 41 (2006) 67–73.
[46] G. Wu, T. Chen, W. Su, G. Zhou, X. Zong, Z. Lei, C. Li, International Journal of Hydrogen Energy 33 (2008) 1243–1251.
[47] W. Cui, C. Xu, S. Zhang, L. Feng, Journal of Photochemistry and Photobiology A: Chemistry 175 (2005) 89–93.
[48] J.R. Hwu, C.Y. Hsu, M.L. Jain, Tetrahedron Letters 45 (2004) 5151–5154.
[49] S. Yan, S.O. Salley, K.Y.S. Ng, Applied Catalysis A 353 (2009) 203–212.
[50] V.E. Henrich, P.A. Cox, The Surface Science of Metal Oxides, Cambridge University Press, Cambridge, 1994.
[51] M. Lopez-Granados, M.D. Zafra-Poves, D. Martin-Alonso, F. Cabello-Galisteo, R. Moreno-Tost, J. Santamaria, J.L.G. Fierro, Applied Catalysis B 73 (2007) 317–329.
[52] G.J. Suppes, K. Bockwinkel, S. Lucas, J.B. Manson, J.A. Heppert, Journal of the American Oil Chemists Society 78 (2001) 139–146.
[53] H.J. Kim, B.S. Kang, M.J. Kim, Y.M. Park, D.K. Kim, J.S. Lee, K.Y. Lee, Catalysis Today 93 (2004) 315–320.
[54] E. Leclercq, A. Finiels, C. Moreau, Journal of the American Oil Chemists Society 78 (2001) 1161–1165.
[55] G.L. Suppes, M.A. Dasari, E.J. Doskocil, P.J. Mankidy, M.J. Goff, Applied Catalysis A 257 (2004) 213–223.
[56] S.W. Robert, A.F. Lee, K. Wlson, Green Chemistry 6 (2004) 199–206.